Acta Crystallographica Section B
Structural Science
ISSN 0108-7681

Disorder and pseudo-symmetry in octakis(trivinylsilyl)octasilicate

Carla Slebodnick,[a]* Ross J. Angel,[b] Brian E. Hanson,[a] Pradyot A. Agaskar,[c] Tatiana Soler[d] and Larry R. Falvello[d]

[a]Virginia Tech Crystallography Laboratory, Department of Chemistry, Virginia Polytechnic Institute and State University, Blacksburg, VA 24061, USA, [b]Virginia Tech Crystallography Laboratory, Department of Geosciences, Virginia Polytechnic Institute and State University, Blacksburg, VA 24061, USA, [c]Spherosils LLC, 2000 Kraft Drive, Suite 1110, Blacksburg, VA 24060, USA, and [d]University of Zaragoza-CSIC, Department of Inorganic Chemistry and Aragon Materials Science Institute, Plaza San Francisco s/n, E-50009 Zaragoza, Spain

Correspondence e-mail: slebod@vt.edu

Received 3 December 2007
Accepted 14 April 2008

Octakis(trivinylsilyl)octasilicate was prepared by capping octaspherosilicate cubes, $[Si_8O_{20}]^{8-}$, with trivinylsilyl groups in methanol solution. Crystals grown from CCl_4 crystallize in the tetragonal space group $I4_1$. Systematic absences are consistent with the space group $I4_1/amd$, although the R_{int} values clearly indicate $4/m$ rather than $4/mmm$ Laue symmetry. Structure solution and refinement show that the pseudo *a*-glide results from the approximate $m\bar{3}m$ symmetry of the core $(Si_8O_{12})O_8^{8-}$ unit. The positions of the molecules conform to a {110} *d*-glide that is broken by the small rotations of all the molecules in the same direction about [001]. Crystals grown from toluene give a diffraction pattern consisting of sharp peaks that can be indexed on the same *ca* 7200 Å^3 unit cell, but with $h + k$ even, and l even only. The l = odd layers contain no Bragg spots, but instead exhibit diffuse sheets of intensity. Within the sheets of diffuse scattering are streaks parallel to $\mathbf{r}^* = \langle 110 \rangle^*$ that cross at the $h + k$ odd Bragg positions. This diffuse scattering pattern arises from well ordered rods of molecules parallel to *c* with frequent faults in the stacking sequence of molecules parallel to $\langle 110 \rangle$, with displacement vectors of $[00\frac{1}{2}]$.

1. Introduction

Polyhedral oligomeric silsequioxane molecules encompass a wide range of closed- and open-shelled organosilicates (Agaskar *et al.*, 1987; Feher & Blanski, 1990; Feher *et al.*, 1989). The subset of these that are comprised of a cube of eight Si atoms with 12 bridging O atoms and eight terminal O atoms, $[Si_8O_{20}]^{8-}$ (Smolin *et al.*, 1979), and capped with a variety of organic groups (Hasegawa *et al.*, 2003) are of considerable interest because of their potential applications as precursors to polymers (Choi *et al.*, 2003; Costa *et al.*, 2001), ceramics (Agaskar, 1992), catalysts (He & Zhang, 2006), membranes (Asuncion & Laine, 2007) and other engineering materials (Agaskar, 1989). The $[Si_8O_{20}]^{8-}$ core has dimensions of approximately 0.5 nm per side, and when each corner is capped with a small organic group such as $Si(CH_3)_3$ the overall dimension is approximately 1 nm per side. Such functionalized $[Si_8O_{20}]^{8-}$ molecules are thus excellent precursors to nanostructured materials (Laine, 2005; Tamaki *et al.*, 2001, 2003; Waddon & Coughlin 2003; Zheng *et al.*, 2002). The title compound, octakis(trivinylsilyl)octasilicate, $[Si(C_2H_3)_3]_8[Si_8O_{20}]$, has the maximum number of vinyl groups on each cube vertex possible in the first generation of a modified cube. Such hyper-functionalized polyhedra are rare and offer unique opportunities for further modification and materials synthesis.

Octakis(trivinylsilyl)octasilicate was prepared by a modification of the method of Hoebbel for the preparation of capped $[Si_8O_{20}]^{8-}$ materials (Hoebbel *et al.*, 1982). Tetra-

methylorthosilicate and tetramethylammonium hydroxide were mixed in methanol to form the cubic $[Si_8O_{20}]^{8-}$ silica core, followed by the addition of trivinylchlorosilane to cap the vertices of the cube (Fig. 1). Crystals were subsequently grown under two different conditions, giving two different, but geometrically related, unit cells. This paper describes the process of solving and refining both of these structures, as an illustration of both pseudo-symmetry and how the structure of a well ordered molecular compound can be used to determine the average structure of its disordered variant.

2. Experimental

Colorless plates were crystallized by slow evaporation of either CCl_4 (cs521) or toluene (cs511) at room temperature. Diffraction data were collected with an Oxford Diffraction Xcalibur diffractometer equipped with a Sapphire 2 CCD detector and Mo $K\alpha$ (λ = 0.71073 Å) radiation, operating at 50 kV and 40 mA. The data-collection routines, unit-cell refinements and data processing were carried out with the program *CrysAlis* (Oxford Diffraction, 2004). The structures were solved by direct methods and refined using *SHELXTL NT* (Sheldrick, 2008), which was also used for molecular graphics generation. Non-H atoms were refined anisotropically and a riding model was used for the H atoms. The final refinement of cs521 included a merohedral twin model for inversion [Flack parameter = 0.59 (13)]. The inability to model a small degree of short-range disorder, evident by a small amount of diffuse scattering parallel to $\mathbf{r}^* = \langle 110 \rangle^*$, is presumably the cause of the slightly unsatisfactory displacement parameters and residual electron density. The final refinement of cs511 included a whole-molecule disorder model that is described in detail below.

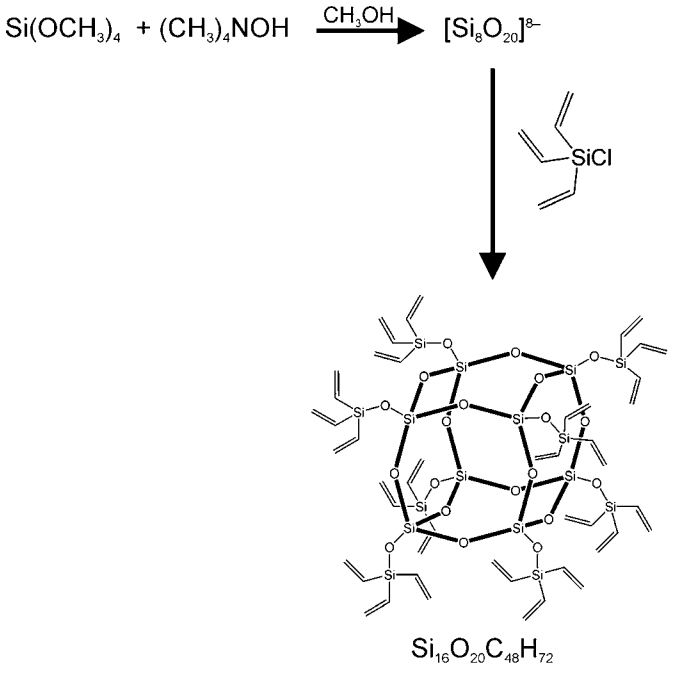

Figure 1
Synthetic scheme for octakis(trivinylsilyl)octasilicate.

3. Results and discussion

3.1. Crystal structure of cs521

Initial screening of the cs521 crystals grown from CCl_4 was very promising. Diffraction peaks were clean and single and the preliminary unit-cell parameters were consistent with a body-centered tetragonal lattice with V = 7197 Å^3 (hereafter referred to as the 7200 Å^3 cell) and Z = 4. Apparent systematic absences suggested $I4_1/amd$ space-group symmetry – a space group that was clearly ruled out by the 4/m Laue symmetry of the diffracted intensities (R_{int} 4/m = 0.08; R_{int} 4/mmm = 0.48). Assuming that the apparent d-glide resulted from pseudo-symmetry, we attempted to solve the structure in $I4_1/a$ with the molecule centered at Wyckoff positions 4(a) or 4(b) of $\bar{4}$ point symmetry (as required by Z = 4). The structure solution obtained in $I4_1/a$ was not satisfactory. The $[Si_8O_{20}]^{8-}$ core could be identified, but the trivinylsilyl arms were disordered and appeared to adopt chemically and sterically unreasonable conformations. The space group $I4_1$ gave a satisfactory solution. Crystallographic details for cs521 are presented in Table 1.[1]

In space group $I4_1$, the asymmetric unit of the structure comprises half of the molecule; the molecules are centered at Wyckoff position 4(a) of multiplicity 4 and the point symmetry 2 generates the other half of each molecule. The c axis of the unit cell is one molecule high and the a and b axes are each 2 molecules wide, giving approximate molecular dimensions $\frac{1}{2}a \times \frac{1}{2}a \times c$ (10.585 × 10.585 × 16.059 Å^3), and a molecular volume of 1799.30 Å^3. The individual molecules in the unit cell are related by the 4_1 and 4_3 axes. The floating z coordinate in space group $I4_1$ was intentionally chosen so that molecules are centered at 0 0 0, $\frac{1}{2}\frac{1}{2}\frac{1}{2}$, 0 $\frac{1}{2}\frac{1}{4}$ and $\frac{1}{2}$ 0 $\frac{3}{4}$. The final refinement for cs521 included a twin model for inversion; the Flack parameter refined to 0.59 (13) so, within uncertainties, the crystal consists of an equal number of both twin orientations. Note that the imposition of an inversion twin on space group $I4_1$ amounts to interchange of the screw axes, such that the 4_1 axes become 4_3 and the 4_3 axes become 4_1, and thus interchange of the z coordinate of the molecule centroids at 0 $\frac{1}{2}$ z and $\frac{1}{2}$ 0 z, from $z = \frac{1}{4}$ to $z = \frac{3}{4}$, and $z = \frac{3}{4}$ to $z = \frac{1}{4}$ respectively (Fig. 2c).

The molecular-point symmetry 2 is dictated by both the trivinylsilyl arms and the Si_8O_{12} core. The Si_8O_{12} core approximates $m\bar{3}m$ point symmetry. The molecular symmetry is reduced to tetragonal point symmetry 4/m by the average $Si_{core}-O-Si_{arm}$ angle of 147 (4)° (Table 2) with all eight trivinylsilyl arms rotated towards the c axis. This makes the molecule substantially longer in the z dimension (Fig. 2a). Mirror symmetry parallel to (001) is broken by further distortion of the trivinylsilyl arms so they are not superimposed when viewed in projection down the c axis (Fig. 2b).

[1] Supplementary data for this paper are available from the IUCr electronic archives (Reference: WS5065). Services for accessing these data are described at the back of the journal.

Table 1
Experimental details.

	cs521	cs511
Crystal data		
Crystallization solvent	CCl_4	Toluene
Chemical formula	$C_{48}H_{72}O_{20}Si_{16}$	$C_{48}H_{72}O_{20}Si_{16}$
M_r	1418.50	1418.50
Cell setting, space group	Tetragonal, $I4_1$	Tetragonal, $I4$
Temperature (K)	100 (2)	100 (2)
a, c (Å)	21.1698 (18), 16.059 (3)	15.0040 (6), 7.9872 (5)
V (Å^3)	7197.2 (16)	1798.08 (15)
Z	4	1
D_x (Mg m^{-3})	1.309	1.311
Radiation type	Mo $K\alpha$	Mo $K\alpha$
μ (mm^{-1})	0.35	0.35
Crystal form, color	Plate, colorless	Plate, colorless
Crystal size (mm)	0.12 × 0.11 × 0.04	0.16 × 0.16 × 0.06
Data collection		
Diffractometer	Oxford Diffraction Xcalibur2	Oxford Diffraction Xcalibur2
Data collection method	φ and ω scans, 50 s per frame	φ and ω scans, 25 s per frame
Absorption correction	None	None
No. of measured, independent and observed reflections	26 352, 10 566, 6414	10 423, 1399, 1394
Criterion for observed reflections	$I > 2\sigma(I)$	$I > 2\sigma(I)$
R_{int}	0.052	0.056
θ_{max} (°)	30.1	30.1
No. and frequency of standard reflections	2 every 50 frames	2 every 50 frames
Intensity decay (%)	< 2	< 2
Refinement		
Refinement on	F^2	F^2
$R[F^2 > 2\sigma(F^2)]$, $wR(F^2)$, S	0.060, 0.137, 0.96	0.061, 0.152, 1.23
No. of reflections	10 566	1399
No. of parameters	380	190
H-atom treatment	Constrained to parent site	Constrained to parent site
Weighting scheme	$w = 1/[\sigma^2(F_o^2) + (0.0571P)^2]$, where $P = (F_o^2 + 2F_c^2)/3$	$w = 1/[\sigma^2(F_o^2) + (0.0665P)^2 + 1.9447P]$, where $P = (F_o^2 + 2F_c^2)/3$
$(\Delta/\sigma)_{max}$	0.001	<0.0001
$\Delta\rho_{max}$, $\Delta\rho_{min}$ (e Å^{-3})	1.15, −0.33	0.34, −0.29
Absolute structure	Flack (1983), 5098 Friedel pairs	NA, Friedels merged
Flack parameter	0.59 (13)	NA
Rogers parameter	< 2%	NA

Computer programs used: *CrysAlis* (Oxford Diffraction, 2004), *SHELXL97* (Sheldrick, 2008).

Somewhat surprisingly, the main factor in reducing the molecular point symmetry from 4 to 2 is not the trivinylsilyl arms, but the difference in $Si_{core}-O_{core}-Si_{core}$ angles (Table 2, Fig. 2*b*). For the molecule centered at $\frac{1}{2}$, $\frac{1}{2}$, 0, the average $Si_{core}-O_{core}-Si_{core}$ angles parallel to *a*, *b* and *c* are 150.1 (11), 143.7 (13) and 151.7 (2)°, respectively. This effectively compresses the Si_8O_{12} core along *b*, giving average $Si_{core}-Si_{core}$ edge distances of 3.105 (11), 3.063 (15) and 3.115 (5) Å, respectively, and molecular point symmetry 2.

The packing diagram of cs521 allows us to identify the pseudo symmetry that caused the space-group ambiguity. For the *a* glide to exist, the molecule must adopt point symmetry $\bar{4}$ (Wyckoff positions *a* or *b* in $I4_1/a$). The pseudo *a* glide thus results from pseudo $\bar{4}$ symmetry of the Si_8O_{12} core. If the space group was $I4_1/amd$ with . . *d* glides, the molecule would sit at Wyckoff position 4(*a*) (origin choice 1) with $\bar{4}m2$ symmetry. In addition to the distortion of the molecule breaking the $\bar{4}m2$ symmetry, the orientation of the molecules in the unit cell, such that every molecule is rotated clockwise *ca* 6.6° about [001], breaks the $\bar{4}m2$ symmetry (Fig. 2). This rotation also breaks both the . *m* . and . . *d* symmetry associated with $I4_1/amd$.

3.2. Diffuse scattering in cs511

The cs511 crystals grown from toluene give raw diffraction images with sharp peaks (*i.e.* Bragg reflections) and streaks of diffuse scattering halfway between the Bragg reflections (Fig. 3*a*). The Bragg reflections can be indexed on the same 7200 Å^3 unit cell as cs521, but all have indices $h + k$ = even and l = even. When cs511 is indexed to the 7200 Å^3 cell, diffuse scattering occurs as two-dimensional sheets in the l = odd planes. These sheets of intensity are consistent with well ordered rods of molecules parallel to *c*, but adjacent rods that are 'randomly' displaced by faults with a displacement vector of $[00\frac{1}{2}]$. Within the sheets of diffuse scattering, the intensity is not uniform. There are higher intensity streaks parallel to $\mathbf{r}^* = \langle 110\rangle^*$ that cross and form diffuse maxima at $h + k$ = odd Bragg positions (Fig. 3*b*). These streaks indicate additional ordering of the rods of molecules to form ordered {110} sheets within the crystal. Complete ordering in this fashion would lead to the development of Bragg reflections at the intersection of the streaks at $h + k$ = odd and l = odd positions, and hence the I lattice, as found in the cs521 crystals. In cs511, however, the ordering is interrupted by $[00\frac{1}{2}]$ displacements at faults between neighboring {110} sheets and this results in the streaks in the diffraction pattern (Fig. 3*b*).

3.3. Crystal structure of cs511

The Bragg spots of cs511 represent the average disordered unit cell, taking into consideration the faults described above. Indexing the Bragg reflections of cs511 gives a unit cell of V = 1798.08 (15) Å^3 (herein referred to as 'the 1800 Å^3 cell') that is geometrically related to 'the 7200 Å^3 cell' of cs521. The transformations between the 7200 Å^3 cell and the 1800 Å^3 cell are described in Table 3 and depicted in Fig. 4(*a*). Table 4

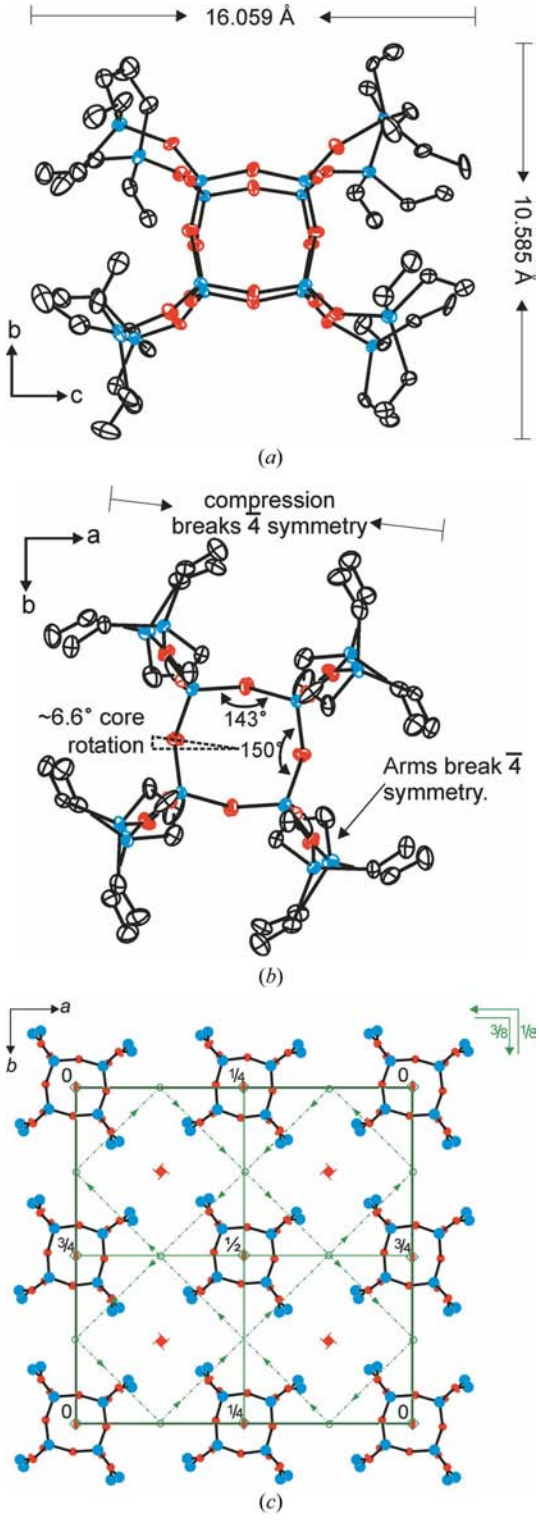

Figure 2
(*a*) Displacement ellipsoid drawing (50%) of cs521 viewed down [100] and depicting the dimensions of the molecule. (*b*) View down [001] depicting the distortions of the Si_8O_{12} core and the trivinylsilyl arms that reduce the molecular point symmetry to 2. (*c*) Packing diagram overlaid on a symmetry diagram for $I4_1$ with pseudo *a* . . . , . *m* . and . . *d* symmetry elements shown in green. Vinyl groups are omitted for clarity. The *z* coordinates of the molecule centroids are given in black. The inversion twin in $I4_1$ amounts to interchange of the screw axes, such that the 4_1 axes become 4_3 and the 4_3 axes become 4_1.

Table 2
Average bond lengths (Å) and angles (°) for cs521 and cs511.

	cs521		cs511	
	Bond direction†	Average	Bond direction	Average
$Si_{core}-O_{core}$	∥⟨100⟩	1.607 (4)	–	1.608 (8)
$Si_{core}-O_{core}$	∥⟨010⟩	1.611 (7)	–	–
$Si_{core}-O_{core}$	∥⟨001⟩	1.606 (10)	–	1.607 (14)
$Si_{core}-O_{core}$	–	1.588 (8)	∥⟨110⟩	1.591 (1)
$O_{arm}-Si_{arm}$	–	1.643 (8)	–	1.628 (1)
$Si_{arm}-C$	–	1.846 (10)	∥⟨001⟩	1.838 (9)
$CH{=}CH_2$	–	1.320 (20)	–	1.29 (3)
Si···Si edge	∥⟨100⟩	3.105 (11)	–	3.089 (4)
Si···Si edge	∥⟨010⟩	3.063 (15)	–	–
Si···Si edge	∥⟨001⟩	3.115 (5)	–	3.110‡
Si···Si face diagonal	⊥⟨100⟩	4.37 (3)	∥⟨110⟩	4.38 (2)
Si···Si face diagonal	⊥⟨010⟩	4.40 (2)	–	–
Si···Si face diagonal	⊥⟨001⟩	4.361 (6)	∥⟨001⟩	4.37 (3)
Si···Si body diagonal	–	6.359 (2)	⊥⟨110⟩	5.262‡
$Si_{core}-O_{core}-Si_{core}$	∥⟨100⟩	150.1 (11)	–	147.7 (15)
$Si_{core}-O_{core}-Si_{core}$	∥⟨010⟩	143.7 (13)	⊥⟨001⟩	–
$Si_{core}-O_{core}-Si_{core}$	∥⟨001⟩	151.7 (2)	–	150.7‡
$Si_{core}-O_{core}-Si_{arm}$	–	147 (4)	∥⟨110⟩	147 (4)
$O_{core}-Si_{core}-O_{core}$	⊥⟨100⟩	109.3 (7)	–	109.4 (8)
$O_{core}-Si_{core}-O_{core}$	⊥⟨010⟩	109.5 (9)	∥⟨001⟩	–
$O_{core}-Si_{core}-O_{core}$	⊥⟨001⟩	109.4 (2)	–	109.2 (7)
$O_{core}-Si-O_{arm}$	∥⟨100⟩	109.9 (9)	⊥⟨110⟩	110.4 (14)
$O_{core}-Si-O_{arm}$	∥⟨010⟩	110.1 (10)	–	–
$O_{core}-Si-O_{arm}$	∥⟨001⟩	108.6 (7)	⊥⟨001⟩	108.1 (6)
$O_{arm}-Si_{arm}-C$	–	108.0 (11)	∥⟨110⟩	107.6 (14)
C—Si—C	–	110.9 (13)	–	111.3 (13)
Si—C═C	–	124.6 (14)	∥⟨001⟩	126 (3)

† All directions are defined relative to the molecule centered at $\frac{1}{2}\,\frac{1}{2}\,0$ in the 7200 Å^3 cell. ‡ There is only one value in this category so the standard uncertainty could not be calculated.

describes the diffuse scattering pattern relative to both cell settings.

The Laue symmetry and systematic absences of cs511 in the 1800 Å^3 cell are consistent with space groups $I4/m$, $I\bar{4}$ or $I4$ and $Z = 1$. A value of $Z = 1$ is not reasonable for a tetragonal I lattice unless there is whole-molecule disorder with equivalent positions at 0,0,0+ and $\frac{1}{2},\frac{1}{2},\frac{1}{2}$+, each of 50% occupancy. Fortunately, whole-molecule disorder is consistent with the observed diffuse scattering pattern in cs511. In the ensuing discussion we begin with the ordered cs521 structure in the 7200 Å^3 cell, apply the $[00\frac{1}{2}]$ fault vectors on {110} fault planes to build a model disordered structure and ultimately obtain a refined structure for cs511 in the 1800 Å^3 unit cell.

Fig. 4(*b*) shows a schematic of the cs521 structure overlaid on an $I4_1$ symmetry diagram. Each rectangle represents one $C_{48}H_{72}O_{20}Si_{16}$ molecule and is intended to emphasize the point symmetry 2 and the non-overlapping trivinylsilyl arms. Although the *z* coordinates are not crystallographically constrained in $I4_1$, for convenience we have defined the *z* coordinates so that one of the molecules is centered at the origin. To understand the effect of the faults parallel to {110} (depicted in green in Fig. 4*b*), concentrate on the molecules labelled *A* and *B*, and centered at 0,0,0 and $0,\frac{1}{2},\frac{1}{4}$, respectively. The displacement of $[00\frac{1}{2}]$ across the fault causes the centroid

of A to shift to $0,0,\frac{1}{2}$ and the centroid of B to shift to $0,\frac{1}{2},\frac{3}{4}$. Assuming that, on average across the entire crystal, the faults cause 50% disorder, the average structure has the A molecules centered at 0,0,0 and $\frac{1}{2}$, and the B molecules centered at $0,\frac{1}{2},\frac{1}{4}$ and $\frac{3}{4}$, each with 50% occupancy. Applying the $[00\frac{1}{2}]$ fault vector to all of the molecules in the unit cell generates the average structure shown in Fig. 4(*c*). Since the environments at 0,0,0.0 and $0,0,\frac{1}{2}$ are now identical, the unit cell is now best represented by halving the c axis and fixing the occupancies at 50% (Fig. 4*d*). Further examination of the model in Fig. 4(*d*) shows that all of the molecules labeled '*A*' now have exactly equivalent environments, and the cell has become C-face centered. Transformation of this cell to a primitive setting yields the 1800 Å^3 unit cell (blue cell in Fig. 4*d*) obtained from the Bragg reflections of the diffraction pattern for cs511. In this 1800 Å^3 cell, A is centered at 0,0,0 and B is centered at $\frac{1}{2},\frac{1}{2},\frac{1}{2}$, each with 50% occupancy. Also, the original 4_1 axes of the 7200 Å^3 unit cell become 4_2 axes in the disordered 1800 Å^3 cell and the space group becomes $P4_2$.

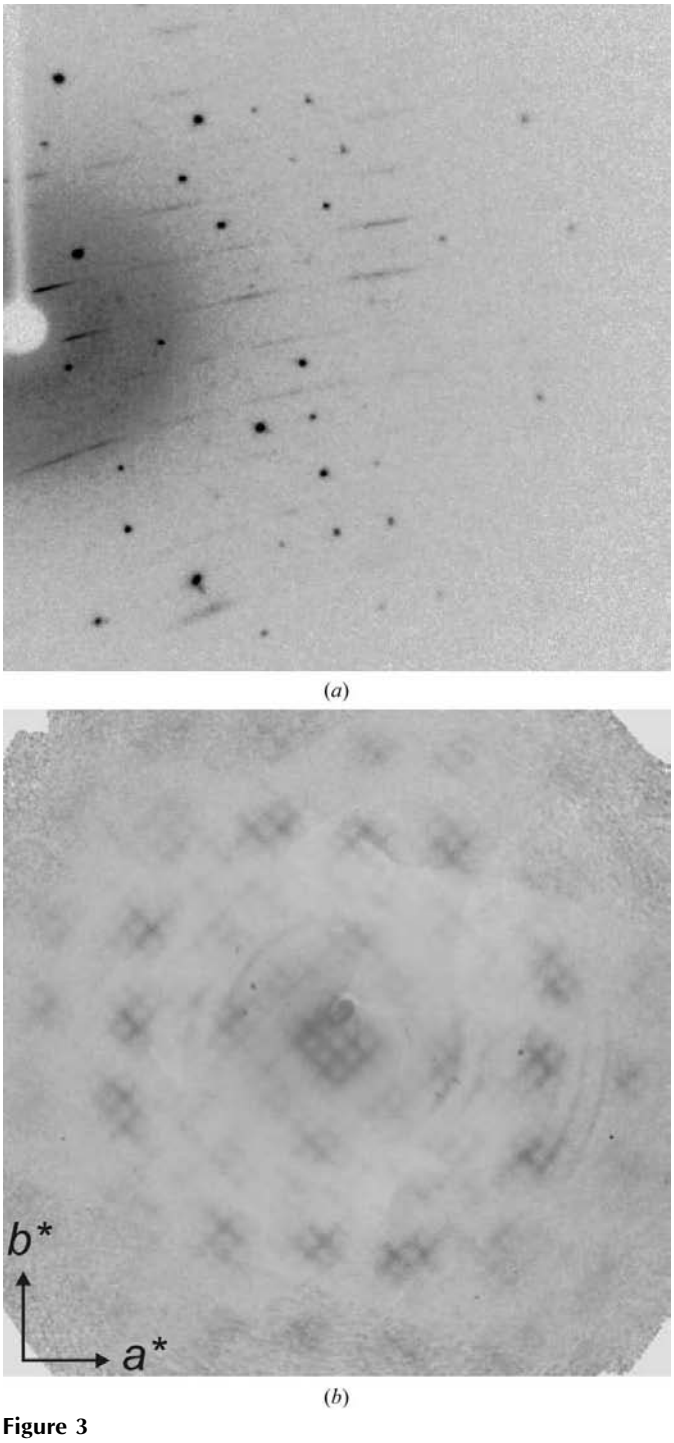

(*a*)

(*b*)

Figure 3
(*a*) Sample CCD image showing the diffuse scattering halfway between Bragg reflections. (*b*) The *hk*5 layer illustrating the crisscross pattern of diffuse scattering present at the *hkl*, l = odd layers of the 7200 Å^3 cell.

Table 3
Transformations from the 7200 Å^3 cell to the 1800 Å^3 cell.

a	$a_{1800} = 1/2^{1/2} a_{7200}$
c	$c_{1800} = \frac{1}{2} c_{7200}$
V	$V_{1800} = \frac{1}{4} V_{7200}$
Transformation matrices	$\mathbf{T} = \begin{pmatrix} \frac{1}{2} & \frac{1}{2} & 0 \\ -\frac{1}{2} & \frac{1}{2} & 0 \\ 0 & 0 & \frac{1}{2} \end{pmatrix}$ $\mathbf{T}^{-1} = \begin{pmatrix} 1 & -1 & 0 \\ 1 & 1 & 0 \\ 0 & 0 & 2 \end{pmatrix}$
Unit-cell dimensions	$(a\ b\ c)_{1800} = (a\ b\ c)_{7200}\mathbf{T}$
Miller indices	$(h\ k\ l)_{1800} = (h\ k\ l)_{7200}\ \mathbf{T}$
Atomic coordinates	$\begin{pmatrix} x \\ y \\ z \end{pmatrix}_{1800} = \mathbf{T}^{-1} \begin{pmatrix} x \\ y \\ z \end{pmatrix}_{7200}$

Table 4
Description of the diffuse scattering pattern in cs511 relative to the 7200 Å^3 and 1800 Å^3 unit cells.

	7200 Å^3 cell	1800 Å^3 cell
a, c (Å)	21.1698 (18), 16.059 (3)	15.0040 (6), 7.9872 (5)
Indices of Bragg reflections	*hkl*, $h + k$ = even, l = even	*hkl*, $h + k + l$ = even (I lattice)
Diffuse scattering	Sheets in l = odd layers Streaks $\parallel$ **r*** = ⟨110⟩* Streaks cross at $h + k$ = odd	Sheets in $l = n + \frac{1}{2}$ layers Streaks $\parallel$ **r*** = ⟨1$\bar{1}$0⟩* Streaks cross at $h + k = n + \frac{1}{2}$
Fault vector	$00\frac{1}{2}$	001

Recall that the Bragg reflections in cs511 are consistent with space groups $I4$, $I\bar{4}$ or $I4/m$. In the current model (Fig. 4*d*), I-lattice symmetry is broken because A and B, although sitting at 0,0,0 and $\frac{1}{2},\frac{1}{2},\frac{1}{2}$, have different orientations; B is rotated 90° relative to A. To obtain $I4$, $I\bar{4}$ or $I4/m$ from $P4_2$, the molecular point symmetry must be increased to 4, $\bar{4}$ or 4/m, respectively. Assuming only minor distortions, these three point groups are all compatible with the Si_8O_{12} core. When considering the relative orientations of the trivinylsilyl arms, however, only point group 4 is reasonable (Fig. 5*b*). In a projection of the structure of cs521 down [001], note that the O_{arm}–Si_{arm} atoms do not overlay perfectly and that all the upper O_{arm}–Si_{arm} atoms are rotated in the same direction relative to the bottom O_{arm}–Si_{arm} atoms (Fig. 5*a*). Thus, 4/m symmetry is not compatible with a molecular structure derived from that of cs521 unless there is significant rotation of the arms to bring the upper and lower arms into coincidence in this projection (Fig. 5*c*). Imposition of point symmetry $\bar{4}$ onto the molecule inherited from cs521 requires a reversal of the relative rota-

tions of upper and lower arms, as indicated in Fig. 5(*d*). By contrast, point-group symmetry 4 preserves the arrangement of the arms from the structure of cs521 and only has the effect of making some symmetrically equivalent (Fig. 5*b*). Therefore, the space group *I*4 was chosen for cs511.

The point symmetry 4 could be imposed on the molecule by one of two methods:

(i) by increasing the point symmetry of the molecule from 2 to 4 (Fig. 6*a*) or

(ii) by assuming the molecule is of point symmetry 2, but with a 90° rotational disorder about [001] (Fig. 6*b*).

The simpler model of increasing the point symmetry of the molecule to 4 was chosen for the first modeling attempt (Fig. 6*a*). The following steps were used to derive a model for cs511 from the cs521 solution:

(i) The atomic coordinates from cs521 were transformed to the correct coordinates for the 1800 Å^3 cell using the transformation matrix shown in Table 3.

(ii) The effect of the [$00\frac{1}{2}$] fault vectors (relative to the 7200 Å^3 cell) was accounted for by constraining the occupancies at each general position to 50%.

(iii) The molecular point symmetry was increased from 2 to 4. The higher symmetry reduced the number of symmetrically unique atoms from 42 to 21 and the atomic coordinates were averaged accordingly to obtain a starting model.

In this final model, molecules are centered at Wyckoff position 2(*a*), with the floating *z* coordinate chosen so that the molecule is centered at 0,0,0. Note that this effectively places two molecules in the unit cell at 0,0,0 and at $\frac{1}{2},\frac{1}{2},\frac{1}{2}$, but since the occupancies are constrained to 50%, $Z = 1$ in this body-centered lattice.

Refining this model to the Bragg reflections of the 1800 Å^3 cell was very successful, giving *R*1 and *wR*2 values similar to the ordered model (Table 1). Average bond lengths and angles are given in Table 2. Fig. 7(*a*) shows the displacement ellipsoid drawing. The packing diagram (Fig. 7*b*) illustrates the fourfold symmetry of the molecule, the *ca* 6.6° rotation of the molecule and the *I*4 space-group symmetry. There are only very small changes in the molecular geometry between this structure and that of cs521, despite the imposition of higher point symmetry (Table 2). At this point we revisited the possibility that the space group could be *I*4/*m*, which requires molecular point symmetry 4/*m*. The packing diagram down **b** (Fig. 7*b*) clearly demonstrates that the trivinylsilyl arms do not overlap and thus there is no mirror symmetry perpendicular to [001].

Now, consider the diffuse scattering relative to the 1800 Å^3 cell (Table 4). The sheets of diffuse scattering are in the $l = n + \frac{1}{2}$ layers with streaks parallel to **r*** = ⟨100⟩* that cross at the $h + \frac{1}{2}, k + \frac{1}{2}$ Bragg positions. Thus, relative to the 1800 Å^3 cell, the disorder in the stacking sequence of the molecules is along the ⟨100⟩ directions with a fault vector of [001]. Fig. 7(*c*) depicts the average

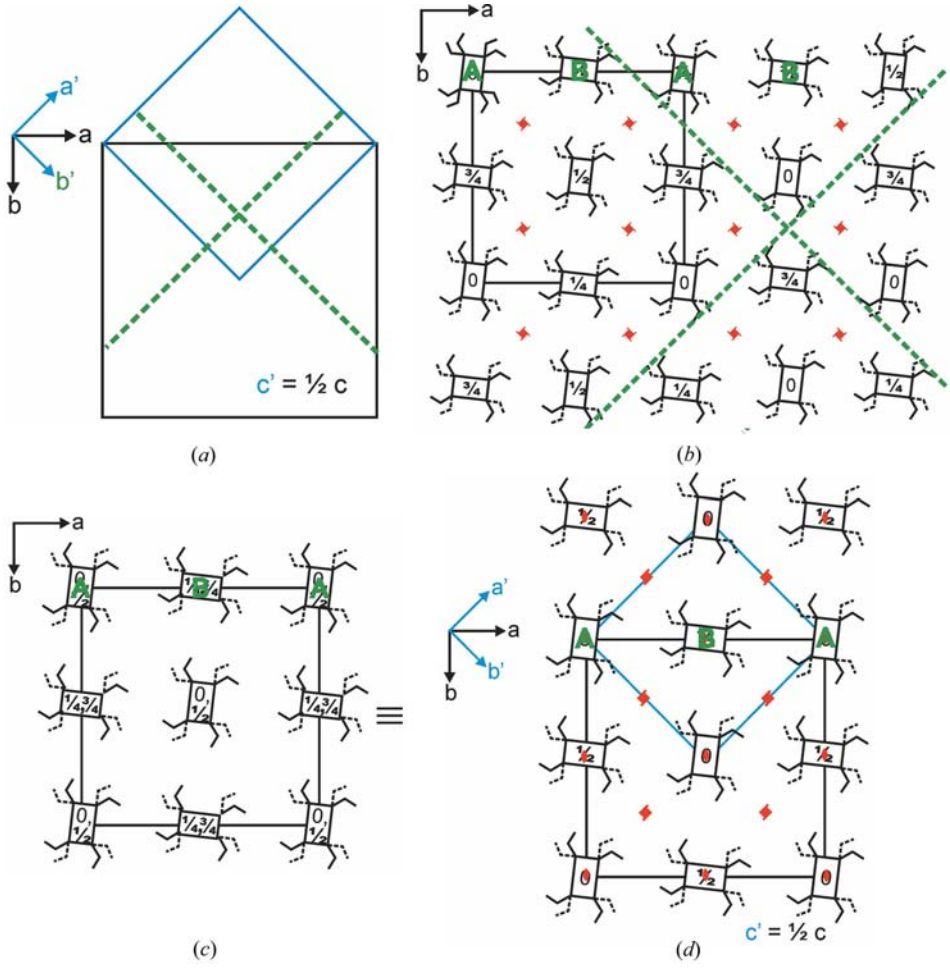

Figure 4
(*a*) Geometric relation between the 7200 Å^3 cell of cs521 (black) and the 1800 Å^3 cell of cs511 (blue). The fault planes (green dotted lines) lie parallel to {110} in the 7200 Å^3 cell, equivalent to {100} in the 1800 Å^3 cell. (*b*) Fault planes overlaid on a schematic of the cs521 structure and depicting {110} fault planes with $00\frac{1}{2}$ displacement across the faults. Each 'armed rectangle' is an exaggerated representation of the point symmetry 2 of the molecule. (*c*) Average structure overlaid on the 7200 Å^3 cell and assuming 50% disorder caused by the $00\frac{1}{2}$ fault. (*d*) Average structure overlaid on the 1800 Å^3 cell (blue) and the 7200 Å^3 cell (black). There is 50% occupancy at each site. The symmetry elements correspond to the space group $P4_2$ for the 1800 Å^3 cell.

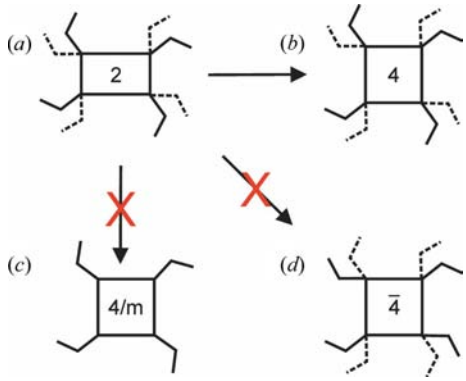

Figure 5
An exaggerated schematic representation of possible (but exaggerated) Si_8O_{12} core symmetries and orientations of the trivinylsilyl arms, as viewed down [001]. Upper trivinylsilyl arms are solid; lower arms are dashed. (*a*) In the cs521 model of point symmetry 2, all upper arms are rotated in the same direction compared with the lower arms. (*b*) Increasing the symmetry from 2 to 4 maintains the topology of the trivinylsilyl arms. (*c*) Increasing the symmetry to 4/*m* requires significant distortion so that the upper and lower arms overlay. (*d*) Increasing the symmetry to $\bar{4}$ requires a change in arm topology, with alternate upper arms rotated in opposite directions.

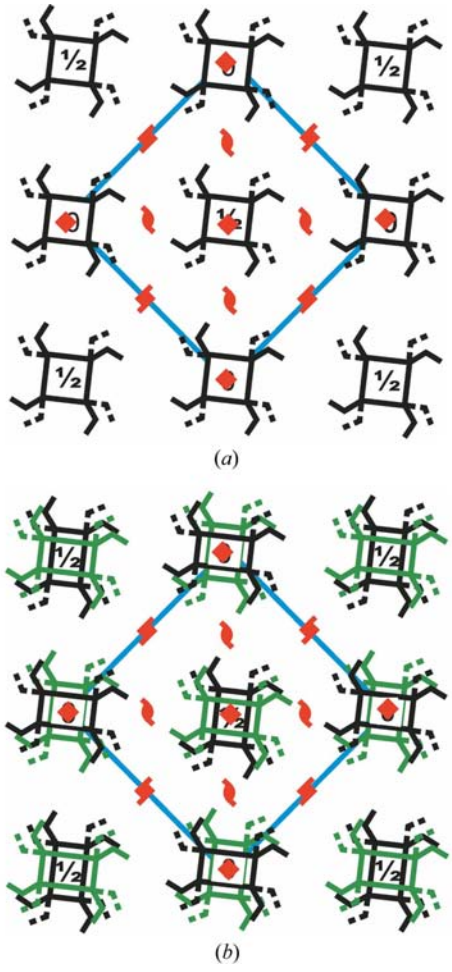

Figure 6
Two possible models that generate a disordered structure with *I*4 symmetry. (*a*) Molecular point symmetry is increased from 2 to 4. There is a 50% occupancy at each site. (*b*) The molecule is disordered *via* a 90° rotation about [001]. The occupancy of each position is 25%.

structure that results from frequent faulting, with apparent interpenetration of adjacent molecules along [001]. This structure is to be interpreted as having a molecule residing at either z = 1, 3, 5, . . . or z = 2 ,4, 6, . . . , therefore, on average,

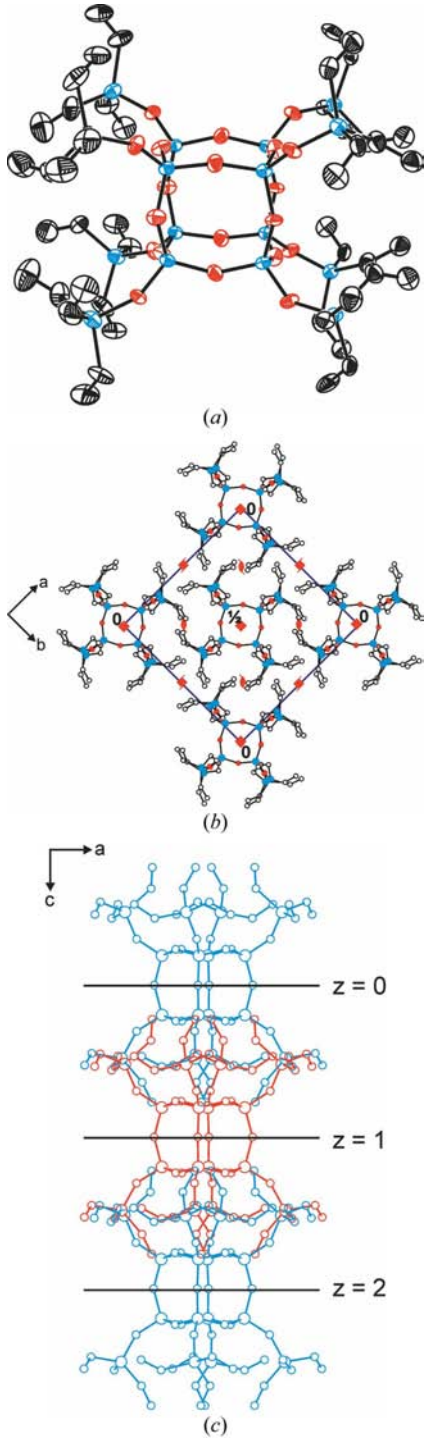

Figure 7
Final model refined to the Bragg reflections for the diffuse scattering sample. (*a*) Displacement ellipsoid drawing at 50% probability. H atoms are omitted for clarity. (*b*) Packing diagram viewed down [001]. (*c*) View along [001] illustrating the disorder resulting from the [001] fault vectors (relative to cs511).

molecules are centered at $z = 1, 2, 3, \ldots$, each 50% of the time and 2, 4, 6, . . . , each 50% of the time.

4. Conclusions

Crystals of $C_{48}H_{72}O_{20}Si_{16}$ have been grown from toluene and CCl_4. It is not clear whether the crystallization solvent determines the structure or whether other subtle differences such as speed of crystallization caused the molecule to crystallize in two different, but related, forms. In the two structures the molecular geometry and the packing differ only slightly, as evidenced by the ability to use the solution from cs521 to calculate the preliminary model for cs511. The structures do differ in the formal point symmetry of the molecules. The molecule in cs521 has point symmetry 2, while the molecule in cs511 has apparent point symmetry 4. It is unclear, and most likely impossible to determine, if the 4 symmetry of cs511 results from 90° rotational disorder of molecules with point symmetry 2 or from the molecules adopting true point symmetry 4. For simplicity, we chose to constrain the cs511 molecule to point symmetry 4 and thereby avoid modelling additional disorder.

The major difference between the two crystal forms is therefore the frequency of the faults within the crystals. In cs521, a twin model successfully reproduced the measured intensity data. To understand this, consider that the $[00\frac{1}{2}]$ fault vectors effectively reverse the direction of the 4_1 and 4_3 screw axes (Fig. 4*b*). The same reversal of the 4_1 and 4_3 screw axes can be obtained by imposition of an inversion twin operation. Therefore, inversion twinning cannot be structurally distinguished from the effect of an isolated fault plane. However, the implicit assumption within a twin model is that there is no significant coherent diffraction from adjacent domains related by the twin operation, and therefore the overall intensity is a function of the sum of the squares of the structure factors, $I(hkl)_{\rm obs} \propto xF(hkl)_1^2 + (1 - x)F(hkl)_2^2$, where the Flack parameter, x, is the fraction of the intensity contribution from each twin. In cs521 the Flack parameter refined to 0.59 (13), indicating approximately equal proportions of the two twin orientations or domains. The success of the twin model to reproduce the measured intensity data indicates that there is long-range order in cs521, and thus that the distance between fault planes is relatively large compared with the coherence length of X-rays. In cs511 the faults are much more frequent, as indicated by the strong diffuse scattering. In this case, the total scattering comes from the coherent scattering from adjacent domains. The intensity of the Bragg reflections is a function of the square of the sum of the structure factors, *i.e.* $I(hkl)_{\rm obs} \propto [\frac{1}{2}F(hkl)_1 + \frac{1}{2}F(hkl)_2]^2$, and the intensity data are modelled as a single disordered structure. Thus, both crystal forms are almost identical, except that they differ in the frequency of the faults or, equivalently, the size of the ordered domains of molecules.

We thank the NSF for Grant CHE-0131128 and the Spanish Ministry of Education and Science for Grant CTQ2005-03141.

References

Agaskar, P. A. (1989). *J. Am. Chem. Soc.* **111**, 6858–6859.
Agaskar, P. A. (1992). *J. Chem. Soc. Chem. Commun.* pp. 1024–1026.
Agaskar, P. A., Day, V. W. & Klemperer, W. G. (1987). *J. Am. Chem. Soc.* **109**, 5554–5556.
Asuncion, M. Z. & Laine, R. M. (2007). *Macromolecules*, **40**, 555–562.
Choi, J., Yee, A. F. & Laine, R. M. (2003). *Macromolecules*, **36**, 5666–5682.
Costa, R. O. R., Vasconcelos, W. L., Tamaki, R. & Laine, R. M. (2001). *Macromolecules*, **34**, 5398–5407.
Feher, F. J. & Blanski, R. L. (1990). *J. Chem. Soc. Chem. Commun.* pp. 1614–1616.
Feher, F. J., Newman, D. A. & Walzer, J. F. (1989). *J. Am. Chem. Soc.* **111**, 1741–1748.
Flack, H. D. (1983). *Acta Cryst.* A**39**, 876–881.
Hasegawa, I., Ino, K. & Ohnishi, H. (2003). *Appl. Organomet. Chem.* **17**, 287–290.
He, F. A. & Zhang, L. M. (2006). *Nanotechnology*, **17**, 5941–5946.
Hoebbel, D., Garzo, G., Ujszaszi, K., Engelhardt, G., Fahlke, B. & Vargha, A. (1982). *Z. Anorg. Allg. Chem.* **484**, 7–21.
Laine, R. M. (2005). *J. Mater. Chem.* **15**, 3725–3744.
Oxford Diffraction Ltd (2004). *CrysAlis*, Version 171.10. Oxford Diffraction Ltd, Abingdon, Oxfordshire, England.
Sheldrick, G. M. (2008). *Acta Cryst.* A**64**, 112–122.
Smolin, Y. I., Shepelev, Y. F., Pomes, R., Hoebbel, D. & Wicker, W. (1979). *Kristallografiya*, **24**, 38–44.
Tamaki, R., Choi, J. W. & Laine, R. M. (2003). *Chem. Mater.* **15**, 793–797.
Tamaki, R., Tanaka, Y., Asuncion, M. Z., Choi, J. W. & Laine, R. M. (2001). *J. Am. Chem. Soc.* **123**, 12416–12417.
Waddon, A. J. & Coughlin, E. B. (2003). *Chem. Mater.* **15**, 4555–4561.
Zheng, L., Waddon, A. J., Farris, R. J. & Coughlin, E. B. (2002). *Macromolecules*, **35**, 2375–2379.